

# SANDIA REPORT

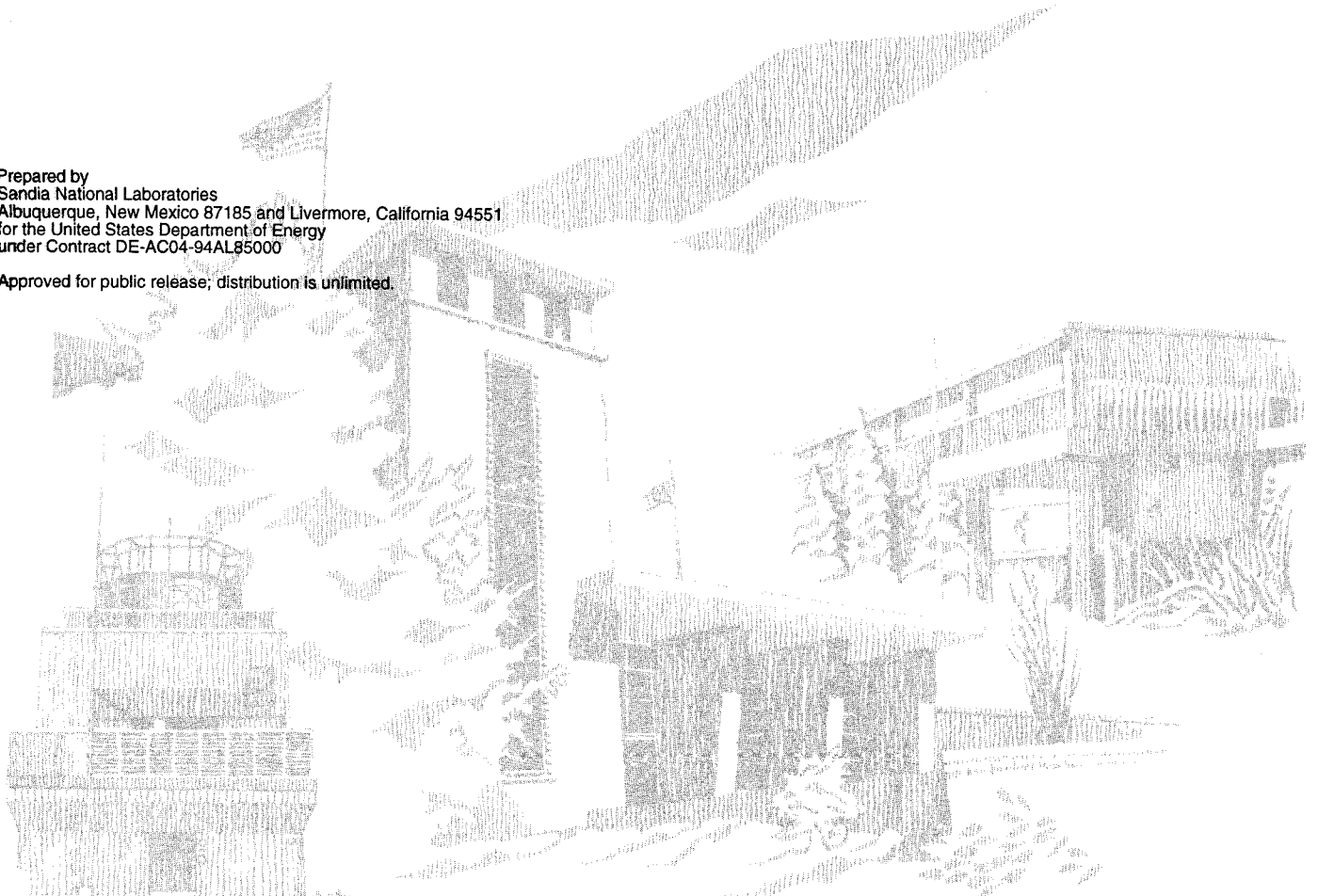
SAND96-8254 • UC-1409  
Unlimited Release  
Printed October 1996

## Increasing the Chemical Content of Turbulent Flame Models Through the Use of Parallel Computing

C. G. Yam, R. Armstrong, M. L. Koszykowski, J. Y. Chen, and M. N. Bui-Pham

Prepared by  
Sandia National Laboratories  
Albuquerque, New Mexico 87185 and Livermore, California 94551  
for the United States Department of Energy  
under Contract DE-AC04-94AL85000

Approved for public release; distribution is unlimited.



Issued by Sandia National Laboratories, operated for the United States Department of Energy by Sandia Corporation.

**NOTICE:** This report was prepared as an account of work sponsored by an agency of the United States Government. Neither the United States Government nor any agency thereof, nor any of their employees, nor any of the contractors, subcontractors, or their employees, makes any warranty, express or implied, or assumes any legal liability or responsibility for the accuracy, completeness, or usefulness of any information, apparatus, product, or process disclosed, or represents that its use would not infringe privately owned rights. Reference herein to any specific commercial product, process, or service by trade name, trademark, manufacturer, or otherwise, does not necessarily constitute or imply its endorsement, recommendation, or favoring by the United States Government, any agency thereof or any of their contractors or subcontractors. The views and opinions expressed herein do not necessarily state or reflect those of the United States Government, any agency thereof or any of their contractors or subcontractors.

This report has been reproduced from the best available copy.

Available to DOE and DOE contractors from:

Office of Scientific and Technical Information  
P. O. Box 62  
Oak Ridge, TN 37831

Prices available from (615) 576-8401, FTS 626-8401

Available to the public from:

National Technical Information Service  
U.S. Department of Commerce  
5285 Port Royal Rd.  
Springfield, VA 22161

SAND96-8254  
Unlimited Release  
Printed October 1996

## **Increasing the Chemical Content of Turbulent Flame Models Through the Use of Parallel Computing**

C. G. Yam, R. Armstrong, and M. L. Koszykowski,  
Sandia National Laboratories/California

J. Y. Chen,  
University of California, Berkeley  
Berkeley, California

and  
M. N. Bui-Pham  
Ernest Orlando Lawrence National Laboratory  
Berkeley, California

### **Abstract**

This report outlines the effort to model a time-dependent, 2-dimensional, turbulent, nonpremixed flame with full chemistry with the aid of parallel computing tools. In this study, the mixing process and the chemical reactions occurring in the flow field are described in terms of the single-point probability density function (PDF), while the turbulent viscosity is determined by the standard  $k$ - $\epsilon$  model. The initial problem solved is a H<sub>2</sub>/Air flame whose chemistry is described by 28 elementary reactions involving 9 chemical species.

## ACKNOWLEDGMENT

This work was supported by the Sandia LDRD program.

## CONTENTS

	<u>Page</u>
Introduction.....	7
Governing Equations.....	9
Scalar PDF Model.....	11
Numerical Method	
Numerical Scheme.....	13
Pressure solver.....	13
Initial and boundary conditions.....	15
Stability.....	16
Parallel computing using POET tool-kit.....	16
Problem of Interest.....	17
Conclusion.....	18
Future Work.....	18
Appendix	
Hydrogen-air mechanism.....	19
References.....	20

## LIST OF FIGURES

		<u>Page</u>
Figure 1.	Mean temperature contours for a turbulent jet flame at time equals to 0.032 second.	22
Figure 2.	Mean density contours for a turbulent jet flame at time equals to 0.032 second.	23
Figure 3.	Mean velocity vectors and stream lines for a turbulent jet flame at time equals to 0.032 second.	24

## Introduction

Manufacturing processing often involves combustion. American industry uses combustion to generate power, to supply heat, or to destroy wastes. Although these various applications employ combustion devices of different geometries and scales, they generally involve turbulent flames. Each of these industries would benefit from optimizing combustion processes and devices to achieve enhanced energy or power generating capabilities, while diminishing the production of criteria pollutants and air toxics. In the past decade, combustion models have been used as design tools, to establish performance, and for marketing applications. The development of robust combustion models is a challenging but worthwhile effort because models can help in design by allowing us to determine the efficient generation of energy from combustion while minimizing the emissions of pollutants.

Modeling of non-reacting, low-Mach number, unsteady flows is a difficult task due to the elliptic nature of the governing equations. When coupled with chemical reactions, the flow is further characterized by multiple time and spatial scales associated with chemical kinetics, which renders the problem even more formidable. Not only does one need to resolve the fluid time scale, but it is also necessary to resolve the chemical time scale. Therefore, one of the most challenging problems in turbulent combustion modeling is to approximate correctly the coupling between reactive and diffusive processes on the smallest scales. Future progress in combustor design (for problems such as pollutant formation, ignition, and extinction) is very promising if modeling capabilities are extended further so that details at a finer level of structure can be predicted. The success of the models as predictive tools for species concentrations requires that they include chemistry, fluid mechanics, and their interactions over a broad range of time and length scales. Our goal is particularly ambitious because it requires the inclusion of very comprehensive chemical mechanisms in the models, which in turn, amplify considerably the computational burden.

For fuels involving fast chemistry (hydrogen is an excellent example for subsonic flows), it is often satisfactory to assume that the chemical kinetics is in equilibrium to avoid the solution of the energy and species equations [1]. For most hydrocarbon fuels, however, the equilibrium assumption produces a flame temperature 10 percent greater than that obtained from a finite-rate chemistry calculation. As the molecular weight of the hydrocarbon fuel increases, results from equilibrium and finite-rate kinetics calculations deviate further. This is because as the molecules become more complex, more intermediate reaction steps are needed to reach the final products, each one of which requires finite time. Calculations of unsteady reacting flows, burning hydrocarbon fuels involving finite-rate chemistry, will be limited as to the type of flow and chemistry they can simulate realistically even with the most powerful serial supercomputers.

Previous numerical studies [2, 3] of unsteady flames have been initialized with a uniform flow condition within the domain of interest. Variations in temperature and

density are then slowly introduced into the simulation. This type of calculation avoids the development of the flame, which is difficult to simulate. This is because the velocity field has an initial value of zero magnitude everywhere, and it is subject to a rapid change in density (e.g., by a factor of seven) resulting from the flame front propagating down-stream. The numerical scheme must be accurate and stable enough to resolve the rapid changes of the flow field. The present goal is to develop a time-dependent numerical code that is capable to predict the formation and development of a turbulent reacting jet where the density changes are vigorous both in space and in time.

In modeling turbulent combustion systems, it is useful to classify the problem in separate regimes such as the distributed-reaction regime or the reaction-sheet regime [4]. This classification is based on a non-dimensional parameter called the Damköhler number, which is defined as the ratio of the flow time to the chemical time. For turbulent combustion, the flow time is usually the turnover time of the smallest eddy (Kolmogorov scale), and the chemical time is the representative time of the entire chemical process. In the large-Damköhler-number or the reaction-sheet regime, the chemistry is fast compared to the fluid dynamics, and the reactions can be considered to occur only in thin sheets where the fuel and oxidizer diffuse into each other. The intractability of direct numerical simulations of turbulent combustion problems with comprehensive chemistry due to the difference in time scales has sparked interest in approximation methods to describe the fluid-chemistry interaction. In the limit of infinite Damköhler number, where chemical equilibrium is maintained, the mixing process can be described as a function of the mixture fraction, and probability density functions are often useful in describing the coupled relationship. An expression for the evolution of a joint-scalar probability density function can be derived to represent the interaction between the turbulent and molecular transport and the chemical reaction.

The model is composed of three parts: the mean turbulent motion, the chemical reaction, and the coupling between chemistry and fluid mechanics. For turbulent reacting flows, direct numerical simulations from first principles are not feasible at practical Reynolds numbers because the length scale of the turbulence, the Kolmogorov scale, decreases proportionally to  $Re^{-9/4}$ , where  $Re$  is the Reynolds number based on the large motion characteristics of the flow. In this study, the mixing process and the chemical reactions occurring in the flow field are described in terms of the single-point probability density function  $\tilde{P}$  while the standard  $k-\epsilon$  model is used to determine the turbulent viscosity. The evolution of chemical kinetics is computed by the probability density function (PDF) [5, 6, 7] method in which the Monte-Carlo simulation describes the turbulent transport of PDF statistical events to and from nearest-neighbor cells and the molecular mixing at the local grid cell. The molecular mixing is a result of both fluid-mechanical turbulence and Fickian diffusion and is currently described by the modified Curl's model [8, 9, 10]. The chemical kinetics need to be computed for each event. This portion of the computations account for 99.3% of the computer time, even with one-step chemistry [11], making this problem particularly amenable to parallel computing. Since

the computational requirements increase roughly linearly with the number of reactive species, the demand of computing power will be severe for complex chemistry.

Combustion chemistry is a complex and active area of research, and in the past 2 decades great strides have been made in the development of chemical kinetic mechanisms for hydrogen and simple hydrocarbons. Detailed mechanisms reported sometimes consist of more than one thousand elementary reactions, as in the case for ignition problems [12]. Over the last several years, reduced mechanisms have become popular and useful in many analytical and computational studies, especially in turbulent combustion research [13, 14]. In reducing a mechanism, various chemical pathways are deemed unimportant and discarded. This is typically accomplished by considering a variety of model flames. While reduced mechanisms provide insight into the more global nature of the chemistry, the discarded pathways could become important in turbulent flames due to the large scale mixing. If the critical pathways were eliminated from the mechanism, the model would fail to reproduce experimental behavior. Nevertheless, for 2-D or 3-D applications in combustion science and technology, one-step or reduced chemistry approaches are used nearly exclusively at the present to make solutions possible within realistic computing times [12]. The advantage of reduced chemistry is that the formulation for the problem is greatly simplified. However, no extrapolation is possible to other experimental conditions, and sometimes interpolations are dangerous because the rate parameters are empirical quantities. A different approach is to use a detailed reaction mechanism; unfortunately, these sets can be quite large, and the evaluation of the chemical reaction rates is computationally intensive. This demand for computational resources necessitates the use of parallel computing to enable our calculations.

### Governing Equations

For very low speed (subsonic) flows ( $\bar{u}_\infty \ll a$ , where  $\bar{u}_\infty$  is the characteristic velocity and  $a$  is the local sound speed), it can be shown that the momentum equation will approach a singular point when the Mach number ( $M$ ) approaches zero. One method of solving this problem is to decompose all variables into a power series of  $\epsilon$ , where  $\epsilon \sim M^2$ , and is assumed to be smaller than one. The decomposed variables are then substituted back into the governing equations. Terms of similar magnitude are then collected. The mean pressure field can be split into the mean thermodynamic pressure (which is constant in space and is defined by the equation of state) and the mean dynamic pressure (which appears in the momentum equation):

$$\bar{P}_{Total} = \bar{P}_{Thermal} + \bar{P}_{Dynamic} \quad (1)$$

with

$$\bar{P}_{Thermal} = \bar{\rho}R\bar{T} \quad (2)$$

where  $\bar{\rho}$  is the mean density, and  $\bar{T}$  is the mean temperature.

I. Continuity Equation:

$$\partial_t \bar{\rho} + \partial_\alpha (\bar{\rho} \tilde{v}_\alpha) = 0 \quad (3)$$

where  $t$  is time, and  $\tilde{v}_\alpha$  is the density weighted velocity vector.

II. Momentum Equation:

$$\bar{\rho} \partial_t \tilde{v}_\alpha + \bar{\rho} \tilde{v}_\beta \partial_\beta \tilde{v}_\alpha = -\partial_\alpha \bar{P} + \partial_\beta (\bar{\tau}_{\alpha\beta} - \langle \rho v_\alpha v_\beta \rangle) + \bar{\rho} g_\alpha \quad (4)$$

where  $\bar{P}$  is the mean dynamic pressure,  $g_\alpha$  is the gravitational vector,  $\bar{\tau}_{\alpha\beta}$  is the laminar stress tensor:

$$\bar{\tau}_{\alpha\beta} = \mu (\partial_\beta \tilde{v}_\alpha + \partial_\alpha \tilde{v}_\beta - \frac{2}{3} \delta_{\alpha\beta} \partial_\gamma \tilde{v}_\gamma) \quad (5)$$

and  $-\langle \rho v_\alpha v_\beta \rangle$  is the Reynolds stresses:

$$-\langle \rho v_\alpha v_\beta \rangle = \mu_t (\partial_\beta \tilde{v}_\alpha + \partial_\alpha \tilde{v}_\beta) - \frac{2}{3} \delta_{\alpha\beta} (\bar{\rho} \tilde{k} + \mu_t \partial_\gamma \tilde{v}_\gamma) \quad (6)$$

III. Turbulent Kinetic Energy Equation:

$$\bar{\rho} \partial_t \tilde{k} + \bar{\rho} \tilde{v}_\beta \partial_\beta \tilde{k} = \partial_\beta \left[ \left( \frac{\mu_t}{\sigma_k} + \mu \right) \partial_\beta \tilde{k} \right] + G - \frac{\mu_t}{\bar{\rho}^2} (\partial_\beta \bar{\rho} \partial_\beta \bar{P}) - \bar{\rho} \tilde{\epsilon} \quad (7)$$

IV. Dissipation Rate Equation:

$$\bar{\rho} \partial_t \tilde{\epsilon} + \bar{\rho} \tilde{v}_\beta \partial_\beta \tilde{\epsilon} = \partial_\beta \left[ \left( \frac{\mu_t}{\sigma_\epsilon} + \mu \right) \partial_\beta \tilde{\epsilon} \right] + C_1 \frac{\tilde{\epsilon}}{\tilde{k}} \left( G - \frac{\mu_t}{\bar{\rho}^2} (\partial_\beta \bar{\rho} \partial_\beta \bar{P}) \right) - C_2 \bar{\rho} \frac{\tilde{\epsilon}^2}{\tilde{k}} \quad (8)$$

where the turbulent viscosity is defined as:

$$\mu_t = C_\mu \bar{\rho} \frac{\tilde{k}^2}{\tilde{\epsilon}} \quad (9)$$

with the gradient-diffusion model for the production of turbulent energy as:

$$G = -\langle \rho v_\alpha'' v_\beta'' \rangle \partial_\beta \tilde{v}_\alpha. \quad (10)$$

The constants for the turbulent model are  $C_\mu=0.09$ ,  $C_1=1.44$ ,  $C_2=1.92$ ,  $\sigma_k = 1.0$ , and  $\sigma_\epsilon = 1.3$ .

### Scalar PDF Model

The single-point probability density function (PDF) equation  $\tilde{P}(\psi_1, \dots, \psi_N; x_i, t)$  of the thermo-chemical variables (scalars)  $\phi_1, \dots, \phi_N$  (where  $1, \dots, N-1$  represent the mean mass fraction of species  $I$ , and  $N$  is the enthalpy of the mixture) is originally developed in Ref. [15]. The resulting equation is written as [15, 16]:

$$\begin{aligned} \bar{\rho} \partial_t \tilde{P} + \bar{\rho} \tilde{v}_\alpha \partial_\beta \tilde{P} + \bar{\rho} \sum_{i=1}^N \partial_{\psi_i} \{ S_i(\psi_1, \dots, \psi_N) \tilde{P} \} = \\ - \partial_\alpha \left( \bar{\rho} \langle v_\alpha'' | \phi_i = \psi_i \rangle \tilde{P} \right) - \bar{\rho} \sum_i^N \sum_j^N \partial_{\psi_i \psi_j}^2 \left( \langle \epsilon_{ij} | \phi_k = \psi_k \rangle \tilde{P} \right) \end{aligned} \quad (11)$$

where  $v_\alpha'' \equiv v_\alpha - \tilde{v}_\alpha$  and  $\epsilon_{ij} = \Gamma \nabla \phi_i \cdot \nabla \phi_j$  with  $\Gamma_i = \Gamma_j = \Gamma$ .

The first term is the time evolution for the PDF. The second term represents the transport of the single-point PDF,  $\tilde{P}$ , by the mean velocity. The third term is the chemical kinetic sources,  $S_i$ , which acts as convection velocities in the scalar space. All of these terms are in closed form, thus no closure model is required. The first term that appears in the right hand side of Eq. (11) is the turbulent flux term, which is unknown and is modeled by the gradient-flux model for statistical moments as:

$$- \bar{\rho} \langle v_\alpha'' | \phi_i = \psi_i \rangle \tilde{P} \equiv C_s \bar{\rho} \frac{\tilde{k}}{\tilde{\epsilon}} \tilde{v}_\alpha'' \tilde{v}_\beta'' \partial_\beta \tilde{P} \quad (12)$$

The second term on the right hand side is the scalar dissipation term, which is also unknown. The closure for this term was based on the pair-wise interaction of fluid particles [17, 18] and resulted in:

$$-\bar{\rho} \sum_i^N \sum_j^N \partial_{\psi_i \psi_j}^2 \left( \langle \varepsilon_{ij} | \phi_k = \psi_k \rangle \tilde{P} \right) \cong \frac{C_D}{\tau} \left\{ \int_{D_N} \dots \int d\psi' \int_{D_N} \dots \int d\psi'' \tilde{P}(\psi') \tilde{P}(\psi'') \theta(\psi', \psi'' | \psi) - \tilde{P} \right\} \quad (13)$$

where

$$\theta(\psi', \psi'' | \psi) = \prod_{i=1}^N \theta_i(\psi_i', \psi_i'' | \psi_i) \quad (14)$$

with

$$\theta(\psi_i', \psi_i'' | \psi_i) = \begin{cases} \frac{1}{|\psi_i'' - \psi_i'|} & \text{for } \psi_i' \leq \psi_i \leq \psi_i'' \text{ or } \psi_i'' \leq \psi_i \leq \psi_i' \\ 0 & \text{otherwise} \end{cases} \quad (15)$$

and  $C_D=6.0$ . The scalar domain  $D_N$  is the set of all allowable values of  $\{\phi_1, \dots, \phi_N\}$ , and  $\tau$  is the time scale for this process.  $\tau$  is defined as:

$$\tau = \frac{\tilde{k}}{\tilde{\varepsilon}}. \quad (16)$$

The above closure model (13) for the scalar dissipation is a simplified version of the Curl mixing model [19].

Formal mathematical representations of each term in Eq. (11) by their corresponding statistical Monte Carlo procedures are discussed in details by Pope [20]. Here, we present illustrations to describe the stochastic procedures in simulating effects due to each term in Eq. (11). First, the effects of convection by the mean velocity and turbulent flux on the joint PDF,  $\tilde{P}$ , are simulated by moving representative particles in the time and physical space. For a round jet configuration, let the downstream and cross-stream directions be denoted by  $x$  and  $r$ , respectively. If the PDF equation were solved by a five-point explicit finite difference scheme, the PDF at the new time level  $(t+\Delta t)$  can be expressed as the sum of the PDFs at time level  $(t)$  as:

$$\tilde{P}(\psi_1, \dots, \psi_N; x, r, t + \Delta t) = A(I+1, J) \tilde{P}(\psi_1, \dots, \psi_N; x_{I+1}, r_j, t)$$

$$\begin{aligned}
& + A(I-1, J) \tilde{P}(\psi_1, \dots, \psi_N; x_{I-1}, r_j, t) \\
& + A(I, J) \tilde{P}(\psi_1, \dots, \psi_N; x_I, r_j, t) \\
& + A(I, J+1) \tilde{P}(\psi_1, \dots, \psi_N; x_I, r_{j+1}, t) \\
& + A(I, J-1) \tilde{P}(\psi_1, \dots, \psi_N; x_I, r_{j-1}, t)
\end{aligned} \tag{17}$$

where  $A(I+1, J)$ ,  $A(I, J)$ ,  $A(I-1, J)$ ,  $A(I, J+1)$ , and  $A(I, J-1)$  denote the amount of contributions from cells at  $(I+1, J)$ ,  $(I, J)$ ,  $(I-1, J)$ ,  $(I, J+1)$ , and  $(I, J-1)$ . As the joint PDF can be represented by a number of statistical events, the PDF at time  $(t+\Delta t)$  can be characterized by a sum of statistical events from the five cells at time  $(t)$  weighted by their respective contributions. The events are selected randomly from each cell to form the new PDF at the new time.

Simulation of the modified Curl's mixing model [19] by Janicka et al. [17] is performed by selecting randomly a pair of events within a grid cell and mixing them up to a random degree. The number of pairs to be selected is calculated by the product of the mixing frequency defined in Eq. (12) and the time step  $(\Delta t)$ . The chemical reaction then moves all of the particles to new positions in the composition space according to their rate equations.

## Numerical Method

### I) Numerical Scheme

Cylindrical coordinates with a staggered mesh are used in this study. Radial velocity  $\tilde{u}$  and axial velocity  $\tilde{w}$  are defined at the left and right, upper and lower cell surfaces, respectively, while the mean density  $\bar{\rho}$ , mean pressure  $\bar{P}$ , turbulent kinetic energy  $\tilde{k}$ , turbulent dissipation rate  $\tilde{\epsilon}$ , and PDF  $\tilde{P}$  are defined at the cell centers. To minimize numerical diffusion, a second-order upwind scheme [21] is used for the convective terms. Second-order central differencing scheme is used for the diffusion term. First-order backward differencing scheme is used to advance the solution in time. A semi-explicit scheme similar to Kim and Moin [22] is used to solve for the variables at the new time level, but with an iterative scheme to solve for the pressure field at the new time level.

### II) Pressure Solver

The governing equations consist of the continuity equation, two momentum equations for the velocities, and a PDF equation for the species mean mass fraction and enthalpy of the mixture. The density field is obtained from the PDF equation. However,

an explicit equation for the pressure  $P$  does not exist. The method that was used to obtain pressure in this study is a variation of the projection method developed by Chorin [23]. The present method involves solving the momentum equations using predictor-corrector steps as follows:

Step 1: Predictor

By using the velocity and density field at time level  $n$ , and the most current pressure field, with the new density field  $\bar{\rho}^{n+1}$  obtained from the PDF equation, a provisional velocity field  $\hat{v}_\alpha$  is then obtained by:

$$\bar{\rho}^{n+1} \frac{\hat{v}_\alpha - \tilde{v}_\alpha^n}{\Delta t} = -\partial_\alpha P^n - (\bar{\rho} \tilde{v}_\beta \partial_\beta \tilde{v}_\alpha)^n + (\partial_\beta (\bar{\tau}_{\alpha\beta} - \langle \rho v_\alpha v_\beta \rangle))^n + \bar{\rho}^{n+1} g. \quad (18)$$

Step 2: Corrector

Assuming that the pressure correction  $\alpha$  is known such that  $p^{n+1} = p^n + \alpha$ , a corrected velocity  $\tilde{v}_\alpha^{n+1}$  can be determined by:

$$\bar{\rho}^{n+1} \frac{\tilde{v}_\alpha^{n+1} - \hat{v}_\alpha}{\Delta t} = -\bar{\nabla} \alpha. \quad (19)$$

As the numerical solution iterates between Eqs. (18) and (19), the pressure field at the new time level is included in the solution of  $\hat{v}_\alpha$ . (In fact, if the pressure field at the new time level is known, Eq. (19) is eliminated, and the provisional velocity  $\hat{v}_\alpha$  is the new velocity field that satisfies both momentum and continuity at the new time level.)

The next step is to evaluate the pressure correction  $\alpha$  by using the continuity equation.

$$\partial_t \bar{\rho} + \partial_\alpha (\bar{\rho} \tilde{v}_\alpha)^{n+1} = 0. \quad (20)$$

Letting  $\tilde{v}_\alpha^{n+1} = \hat{v}_\alpha + \tilde{v}_{\alpha_c}$ , where  $\hat{v}_\alpha$  is the provisional velocity field obtained from step 1, and  $\tilde{v}_{\alpha_c}$  is the velocity correction necessary to satisfy mass balance, the continuity equation can be rewritten as:

$$\partial_t \bar{\rho} + \partial_\alpha (\bar{\rho}^{n+1} \hat{v}_\alpha) + \partial_\alpha (\bar{\rho}^{n+1} \tilde{v}_{\alpha_c}) = 0. \quad (21)$$

By defining a scalar  $\phi$  such that  $-\partial_\alpha \phi = \bar{\rho}^{n+1} \tilde{v}_{\alpha_c}$  and substituting for  $\tilde{v}_{\alpha_c}$ , a Poisson equation for  $\phi$  is obtained:

$$\partial_t \bar{\rho} + \partial_\alpha (\bar{\rho}^{n+1} \hat{\tilde{v}}_\alpha) = \partial_{\alpha\alpha} \phi . \quad (22)$$

The final step in this method is to relate the scalar  $\phi$  to the pressure correction  $\alpha$  by using step 2 (corrector) in solving the momentum equation. By substituting the definition of  $\tilde{v}_\alpha^{n+1} = \hat{\tilde{v}}_\alpha + \tilde{v}_{\alpha_c}$ , we have

$$\frac{\bar{\rho}^{n+1} \tilde{v}_\beta^{n+1} - (\bar{\rho}^{n+1} \hat{\tilde{v}}_\beta^{n+1} - \bar{\rho} \tilde{v}_{\beta_c})}{\Delta t} = -\partial_\beta \alpha . \quad (23)$$

Then

$$\frac{\bar{\rho} \tilde{v}_{\beta_c}}{\Delta t} = -\partial_\beta \alpha \quad (24)$$

and

$$\frac{\partial_\beta \phi}{\Delta t} = \partial_\beta \alpha \quad (25)$$

or  $\frac{\phi}{\Delta t} = \alpha$  and  $\tilde{v}_{\beta_c} = -\frac{1}{\bar{\rho}^{n+1}} \partial_\beta \phi$ .

### III) Initial and Boundary Conditions

At time equal to zero, the velocity is initialized to zero everywhere. The density is set to that of ambient air. As time elapses, velocity and density are varied according to prescribed values at the inlet boundary. At the outer radial boundary and at the downstream boundary, a free-flow boundary condition is imposed (i.e., the second derivatives of all variables are set equal to zero). Symmetry boundary conditions are imposed at the axis.

Since  $\phi$  is related to the velocity correction, and since the velocity at all boundaries (except at the outflow boundaries) are known, the velocity corrections are equal to zero. This implies that the normal gradient of  $\phi$  is zero. At the outflow boundaries, since we do not know the velocity, special treatment is required. This is done by first applying the Poisson equation to the entire domain:

$$\iiint (\nabla^2 \phi) dV = \iiint \left[ \partial_t \bar{\rho} + \partial_\alpha (\bar{\rho}^{n+1} \hat{v}_\alpha) \right] dV. \quad (26)$$

Applying Gauss' theorem, the above equation becomes:

$$\iint \bar{\nabla} \phi \cdot \bar{n} dA = \iiint \left[ \partial_t \bar{\rho} + \partial_\alpha (\bar{\rho}^{n+1} \hat{v}_\alpha) \right] dV. \quad (27)$$

Since  $\bar{\nabla} \phi \cdot \bar{n} dA$  is zero at the inlet and on the axis, assuming that the gradient of  $\phi$  along the streamlines at the outflow boundaries is a constant, the gradient of  $\phi$  can then be determined by the right hand side of the above equation.

#### IV) Stability

Due to the explicit nature of the numerical scheme, it is necessary to satisfy a stability criterion. There exists a chemical and a fluid time scale for this problem. With the pdf method, the species and the energy equation (where the chemical scale occurs) has been transformed into a system of first order (in time) ordinary differential equations. With the explicit scheme, these system of equations can be integrated without any restrictions other than the desired accuracy of the solution. Thus the only restrictive time scale is that of the fluid time scale. For the fluid field, the only time scale of concern is that of convection. The time step  $\Delta t^n$  is then calculated by:

$$\Delta t^n = \sigma \min_{i,j} \left( \frac{\Delta r_i}{\tilde{u}_{i,j}^n}, \frac{\Delta z_j}{\tilde{w}_{i,j}^n} \right) \quad (28)$$

where  $\sigma$  is the CFL number and is less than unity.

### Parallel computing using POET tool-kit

There has been much interest, in recent years, in parallel computing because of its potential in scientific applications [24]. Frameworks for parallel computing have recently become popular as a potential way to encapsulate and preserve parallel numerical algorithms. Because parallel numerics are orders-of-magnitude more complex and machine dependent than their serial counterparts, the motivation for preserving working implementations is strong. Currently, most practitioners of parallel computations write all of the component numerical code customized for each application. If a new application is to be written, then all of the component numerical operations must be rewritten to suit the new application. Frameworks for parallel computing in general, and

Parallel Object-Oriented Environment and Toolkit (POET) in particular, focus on finding ways to orchestrate cooperation between components implementing the parallel algorithms. POET seeks to be a general platform for scientific parallel algorithm components which can be modified, linked, "mixed and matched" to a user's specification. The purpose of POET is to identify a means for parallel code reuse and to make parallel computing more accessible to scientists whose expertise lies outside the field of parallel computing.

One of the main goals in effective parallel computing is scaleability, i.e., maintaining the speed-up based on the number of processors used. Scaleability enables us to solve more complex problems by employing a larger number of processors, and it cannot be achieved unless the work is distributed evenly among the processors. Unfortunately, the combustion community has not been able to resolve the scaleability issue; therefore, many problems (especially those associated with turbulent combustion) cannot be addressed. The dynamic load balancing [25] module in POET is the means used to facilitate this even distribution at runtime in a parallel system to improve the overall system performance and utilization. Up to now, this method is rarely used outside of the computer science community; however, we have proven the ability to use load balancing in solving combustion problems [11]. Load balancing is even more essential and effective when used in systems where steep gradients exist, such as in a flame or in a heterogeneous computational environment where processors of different capabilities are employed. Without the use of load balancing, some processors may be over-burdened with computations while others remain idle, creating a bottleneck that limits the speed-up.

### **Problem of interest**

In order to test the numerical method, a hydrogen jet, with a mean velocity of 75 m/s and a jet diameter of 5.2mm injected into a slow-moving cold air stream of 1 m/s, is simulated. The outer radius of the computational domain is set at 25 cm, and the downstream outflow boundary is set at 41 cm. A total of 52 by 102 grid points are used in the radial and axial directions.

Historically, turbulent combustion calculations usually employ reduced mechanisms, where the chemistry is represented by a few (from one to four) global reactions. However, since we have the use of POET coupled with parallel computing capability, we can increase the complexity of the flame chemistry so that it can characterize accurately the combustion of Hydrogen in air. The chemical kinetic mechanism used in these H<sub>2</sub>/Air turbulent flame calculations consists of 28 reactions involving 9 chemical species and is shown in Appendix I.

The flow is assumed to be ignited at  $t = 0$  seconds by invoking the equilibrium assumption. The PDF is then used to calculate all of the scalar variables. Figure 1 shows the mean temperature contours at time equal 0.032 seconds after the flow initiated. Due to

the high velocity and high temperature (low density) of the reaction zone, the fluid in this region accelerates and expands rapidly into the cold air region as shown in Fig. 1. Figure 2 shows the mean density contours at the same time. One can clearly see the expansion of the hot hydrogen gas into the surrounding gas. Figure 3 shows the velocity vectors and streamlines at the same time. We can see the fast moving hydrogen jet cuts into the air flow. Due to the high shearing action, a vortex ring is formed right under the flame front. The ability to calculate this transient reacting flow shows that the current method can be used to solve a more complex system of chemistry.

### **Conclusion**

The formation and development of a turbulent hydrogen reacting jet with 9-species has been successfully predicted using the low-Mach number form of the Navier-Stokes equation and the PDF Monte-Carlo method. Free outflow boundary conditions that allow mass to enter or exit the computational domain are employed in this study. This allows the placement of the outer boundary of the computational domain close to the region of interest. For a given number of grid points, it is then more computationally efficient to utilize a relatively fine grid, which reduces numerical dissipation to a minimum. The PDF method enables us to model the effects of turbulence on chemical reactions more accurately. With the use of parallel computing, we can increase the number of chemical species to accommodate hydrocarbons and other pollutants in our models.

### **Future Work**

The next step in our research will be to model  $\text{CH}_4/\text{Air}$  flames with full chemistry. The representative chemical kinetic mechanism for methane/air combustion consists of more than two hundred elementary reactions involving 53 chemical species. Eventually, we will want to include Nitrogen chemistry in our mechanism in order to predict the formation of pollutants such as oxides of Nitrogen such as  $\text{NO}_x$ .

## Appendix 1

### Hydrogen-air mechanism

REACTIONS	A	b	E
1. HO <sub>2</sub> +HO <sub>2</sub> =H <sub>2</sub> O <sub>2</sub> +O <sub>2</sub>	2.5E11	0.0	-1242.0
2. OH+OH+M=H <sub>2</sub> O <sub>2</sub> +M H <sub>2</sub> O/6.5/ H <sub>2</sub> /1.0/ O <sub>2</sub> / 0.4/ N <sub>2</sub> / .4/	3.25E22	-2.0	0.0
3. H <sub>2</sub> O <sub>2</sub> +M=OH+OH+M H <sub>2</sub> O/6.5/ H <sub>2</sub> /1.0/ O <sub>2</sub> / 0.4/ N <sub>2</sub> / .4/	1.692E24	-2.0	48348.0
4. H <sub>2</sub> O <sub>2</sub> +H=H <sub>2</sub> O+OH	1.E13	0.0	3585.0
5. H <sub>2</sub> O <sub>2</sub> +OH=H <sub>2</sub> O+HO <sub>2</sub>	5.4E12	0.0	1003.8
6. H <sub>2</sub> O+HO <sub>2</sub> =H <sub>2</sub> O <sub>2</sub> +OH	1.802E13	0.0	32206.0
7. H <sub>2</sub> O <sub>2</sub> +H=HO <sub>2</sub> +H <sub>2</sub>	4.79E13	0.0	7945.8
8. H+O <sub>2</sub> =OH+O	2.00E14	0.0	16800.0
9. OH+O=H+O <sub>2</sub>	1.568E13	0.0	841.3
10. O+H <sub>2</sub> =OH+H	5.06E4	2.67	6285.9
11. OH+H=O+H <sub>2</sub>	2.222E4	2.67	4371.4
12. OH+H <sub>2</sub> =H <sub>2</sub> O+H	1.00E8	1.6	3298.3
13. H <sub>2</sub> O+H=OH+H <sub>2</sub>	4.312E8	1.6	18274.4
14. 2OH=O+H <sub>2</sub> O	1.5E9	1.14	100.4
15. O+H <sub>2</sub> O=2OH	1.473E10	1.14	16990.9
16. O <sub>2</sub> +H+M=HO <sub>2</sub> +M H <sub>2</sub> O/6.5/ H <sub>2</sub> /1.0/ O <sub>2</sub> / 0.4/ N <sub>2</sub> / .4/	2.3E18	-8	0.0
17. HO <sub>2</sub> +M=O <sub>2</sub> +H+M H <sub>2</sub> O/6.5/ H <sub>2</sub> /1.0/ O <sub>2</sub> / 0.4/ N <sub>2</sub> / .4/	3.19e18	-8	46699.3
18. H+HO <sub>2</sub> =2OH	1.5E14	0.0	1004.0
19. H+HO <sub>2</sub> =H <sub>2</sub> +O <sub>2</sub>	2.5E13	0.0	693.1
20. OH+HO <sub>2</sub> =H <sub>2</sub> O+O <sub>2</sub>	6.0E13	0.0	0.0
21. HO <sub>2</sub> +H=H <sub>2</sub> O+O	3.E13	0.0	1720.8
22. HO <sub>2</sub> +O=OH+O <sub>2</sub>	1.8E13	0.0	-406.3
23. H+H+M=H <sub>2</sub> +M H <sub>2</sub> O/6.5/ H <sub>2</sub> /1.0/ O <sub>2</sub> / 0.4/ N <sub>2</sub> / .4/	1.8E18	-1.0	0.0
24. OH+H+M=H <sub>2</sub> O+M H <sub>2</sub> O/6.5/ H <sub>2</sub> /1.0/ O <sub>2</sub> / 0.4/ N <sub>2</sub> / .4/	2.2E22	-2.0	0.0
25. O+O+M=O <sub>2</sub> +M H <sub>2</sub> O/6.5/ H <sub>2</sub> /1.0/ O <sub>2</sub> / 0.4/ N <sub>2</sub> / .4/	2.9E17	-1.0	0.0
26. OH+O+M=HO <sub>2</sub> +M	1.0E16	0.0	0.0
27. H <sub>2</sub> +O <sub>2</sub> =OH+OH	1.70E13	0.0	47780.0
28. H+O+M=OH+M H <sub>2</sub> O/5/ H <sub>2</sub> /1.0/ O <sub>2</sub> /1.0/ N <sub>2</sub> /1.0/	6.20E16	-0.6	0.0

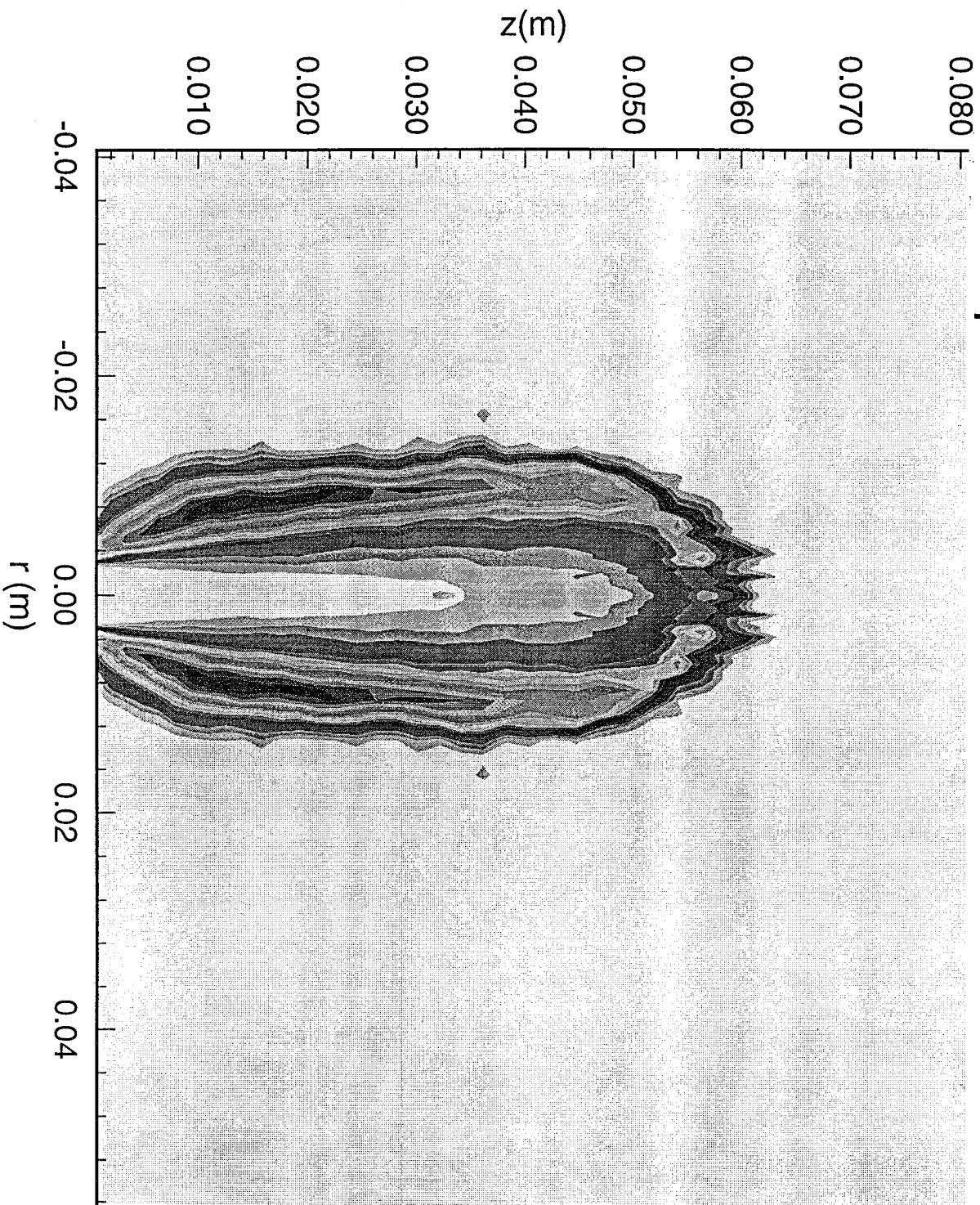
The rate coefficients are in the modified Arrhenius equation,  $k_f = AT^b \exp\left(\frac{E}{RT}\right)$ , where  $A$  is the frequency factor;  $b$  is the temperature exponent;  $E$  is the activation energy;  $R$  is the universal gas constant, and  $T$  is the temperature. The units are moles, cubic centimeters, seconds, Kelvins, and calories/mole.

## References

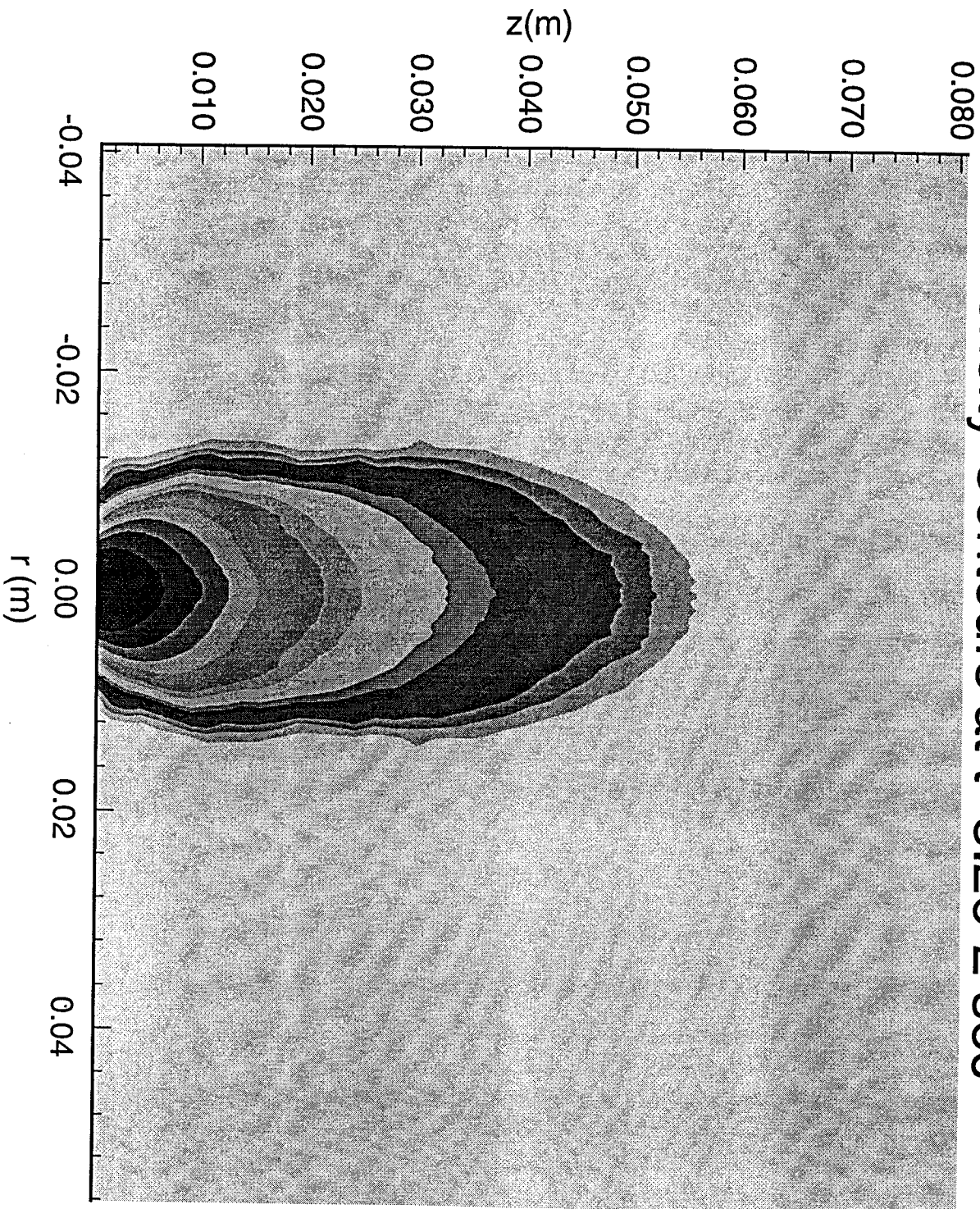
1. Yam, C. 1986. Master Thesis, U.C. Davis.
2. Katta, V.R. and Goss, L.P. and Roquemore, W. M. 1994. *AIAA J.*, **32**, p. 84.
3. Kaplan, C.R., Baek, S.W., Oran, E.S. and Ellzey, J.L. 1994. *Combustion and Flame*, **96**, p. 1.
4. Linan, A. and Williams, F. A. 1993. *Fundamental Aspects of Combustion*. Oxford University Press, New York, Oxford.
5. Pope, S. B. 1981. *Eighteenth Symposium (International) on Combustion*, The Combustion Institute, Pittsburgh, p. 1001.
6. Pope, S. B. 1985. *Prog. Energy Combust. Sci.*, **11**, p. 119.
7. Pope, S. B. 1991. Combustion Modeling Using PDF Methods. *Numerical Approaches to Combustion Modeling*. Edited by E. S. Oran and J. P. Boris. **135**. Progress in Astronautics and Aeronautics. American Institute of Aeronautics and Astronautics, Inc., Washington, D. C.
8. Curl, R. L. 1963. *A. I. Ch. E. Journal*, **9**, p. 175.
9. Janicka, J., Kolbe, W., and Kollmann, W. 1979. *J. Non-Equil. Therm.*, **4**, p. 47.
10. Pope, S. B. 1982. *Combust. Sci. and Tech.*, **28**, p. 131.
11. Koszykowski, M. L.; Armstrong, R. C.; Chen, J. Y.; and Brown, N. J. 1995. Turbulent Jet Flame Modeling with Comprehensive Chemical Kinetics for NO<sub>x</sub> Prediction. Submitted to *J. Comp. Phys*.
12. Warnatz, J. 1992. *Twenty-Second Symposium (International) on Combustion*, The Combustion Institute, Pittsburgh, p. 553.
13. Smooke, M. D., Editor. 1991. *Reduced Kinetic Mechanisms and Asymptotic Approximations for Methane-Air Flames*. Lecture Notes in Physics. Springer-Verlag, Berlin Heidelberg.
14. Peters, N. and Rogg, B. (Editors). 1993. *Reduced Kinetic Mechanisms for Applications in Combustion Systems*. Springer-Verlag, Berlin Heidelberg.

15. Pope, S. B. 1976. *Combustion and Flame*, 27, p. 299.
16. Chen, J-Y., Kollmann, W., Dibble, R.W. 1989. *Combust. Sci. and Technol.*, 64, p. 315.
17. Janicka, J., Kolbe, W., and Kollmann, W. 1979. *J. non-equilib. Thermodyn.*, 4, p. 47.
18. Dopazo, C. 1979. *Phys. Fluids*, 22, p. 20.
19. Curl, R.L. 1963. *A.I.Ch.E.J.*, 9, p. 175.
20. Pope, S.B. 1981. *Combust. Sci. and Technol.*, 25, p. 159.
21. Sharif, M.A.R. and Busnaina, A.M. 1988. *J. Computational Physics*. 74, p. 143.
22. Kim, J and Moin, P. 1985. *J. Computational Physics*. 59, p. 308.
23. Chorin, A.J. 1968. *Math. Computation*. 22, p. 745.
24. Koszykowski, M. L., Armstrong, R. C., Cline, R. E., Macfarlane, J., Brown, N. J., and Chen, J. Y. 1993. The Advanced Combustion Modeling Environment (ACME). *Computing at the leading Edge: Research in the Energy Sciences*. UCRL-TB-111084, U. S. Government Printing Office 1193-785-007, 61.
25. Armstrong, R. C. and Cheung, A. L. 1996. High-Performance Computing Systems Symposium.

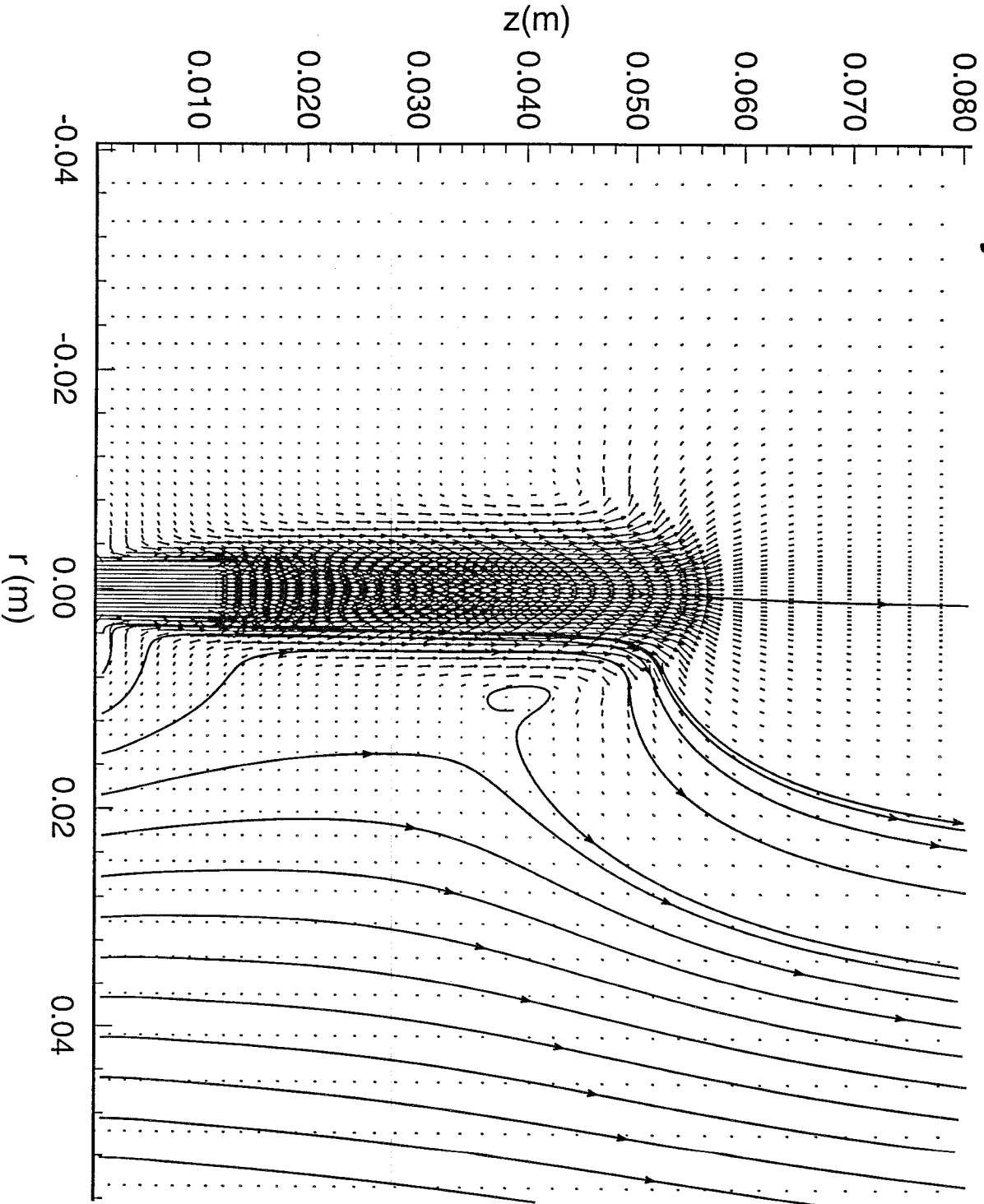
# Temperature Contours at $t=3.2 \times 10^{-2}$ sec



# Density Contours at $t=3.2 \times 10^{-2}$ sec



# Velocity Vector and Streamlines at $t=3.2 \times 10^{-2}$ sec



Unclassified unlimited Release:

- 9001 T. Hunter, 8000  
Attn: J. B. Wright, 2200  
A, West, 8200  
R. C. Wayne, 8400  
P. N. Smith, 8500  
L. A. Hiles, 8800
- 9054 W. J. McLean  
Attn: C. W. Robinson, 8301  
W. Bauer, 8301  
R. W. Carling, 8362  
R. J. Gallagher, 8366
- 9055 F. P. Tully, 8353  
9055 J. L. Durant, 8353  
9055 C. G. Yam, 8353 (2)  
9055 M. N. Bui-Pham, LBNL (2)  
9055 M. L. Koszykowski, 8920  
9021 Technical Communications Department, 8815, for OSTI (10)  
9021 Technical Communications Department, 8815/Technical Library, MS 0899, 4414  
0899 Technical Library, 4414 (4)  
9018 Central Technical Files, 8950-2 (3)